

Investigation of Properties and Characteristics of High-Area-to-Mass Ratio Objects Based on Examples of Optical Observation Data of Space Debris Objects in GEO-like Orbits

Carolyn Früh

*Astronomical Institute, University of Bern, Switzerland,
frueh@aiub.unibe.ch*

Thomas Schildknecht

*Astronomical Institute, University of Bern, Switzerland,
thomas.schildknecht@aiub.unibe.ch*

1 ABSTRACT

The Astronomical Institute of the University of Bern first discovered in 2004 an unexpected population of high area-to-mass ratio (HAMR) objects in GEO-like orbits. Due to their unique properties, these objects pose a major challenge in maintaining an orbit over longer time periods. The orbits of HAMR objects at high altitudes are strongly perturbed by solar radiation pressure. Observations suggest that the objects have are in a tumbling motion state. The Astronomical Institute of the University of Bern (AIUB) has collected a significant set of observations of HAMR objects over the past years. Some of the objects could be followed over longer time intervals.

This paper addresses the task of investigating the properties and characteristics of HAMR objects by analyzing optical observations of five HAMR objects in GEO-like orbits taken from the internal AIUB catalogue. The dynamical properties are investigated by means of systematic orbit determination. Evolution of orbital elements and the area-to-mass ratio over time are evaluated. Differences of orbits determined with observations from a single site or combined observations of various sites are also investigated. The propagated orbits are compared to further optical observations belonging to the same object, which serve as a ground truth.

2 INTRODUCTION

The Astronomical Institute of the University of Bern has maintained a high area-to-mass ratio (HAMR) object catalogue since 2004 and observes HAMR objects on a regular basis. New objects are detected with the one-meter ESA Space Debris Telescope (ESASDT) on Tenerife, Spain, or with the 18 cm ZIMmerwald SMALL Robotic Telescope (ZimSMART), located in Zimmerwald, near Bern, Switzerland. Immediate follow-up observations can be tasked within the night of detection. Both telescopes are also used for regular follow-up observations for catalogue maintenance in addition to the one-meter ZIMmerwald Laser and Astrometric Telescope, located in Zimmerwald, Switzerland, as well. Maintaining a catalogue of HAMR objects is especially challenging due to the unique properties of these objects; regular observations on short time intervals are mandatory. In regular orbit determination, variations in the value of the area-to-mass ratio (AMR) was detected, first investigations were performed, i.e [1]. This paper investigates the dynamical properties in greater detail exemplary through five HAMR objects of the AIUB internal catalogue in geostationary-like orbits. This unique data set of the AIUB permits investigation of the evolution of the orbits over longer time periods. Orbits were determined both with observations of single sites and with combined observations.

3 ORBIT DETERMINATION

All orbits were determined with an advanced version of the CelMech tool [2]. The orbit determination is based on a least squares approach. Earth gravitational potential up to order and degree 12 is used. Earth shadow passes are modeled and corrections due to ocean and Earth tides are taken into account, as well as relativity corrections. Included as solve-for parameters are the area-to-mass ratio (AMR), as well as biases. Biases are parameters that should account for asymmetries of the observed objects, e.g., misalignment of solar panels.

The area-to-mass ratio is derived from the estimated value of the direct radiation pressure (DRP) acceleration:

$$\vec{a} = \frac{C}{2} \times \frac{A_{\oplus}}{|\vec{r} - \vec{r}_{\odot}|^2} \frac{S}{c} \frac{A}{m} \vec{e}_{\odot} \quad (1)$$

\vec{e}_{\odot} is the satellite-Sun direction under consideration of light aberration, $\vec{r} - \vec{r}_{\odot}$ is the direction of the satellite with respect to the Sun, A_{\oplus} is the distance Sun-Earth, one astronomical unit, c is the speed of light, S is the solar radiation flux, and C the reflection coefficient. In the determination of the orbits in this paper, a value of $C = 2.0$ was assumed, which

Table 1: Internal name, eccentricity, inclination (deg), semi major axis (km), area to mass ratio (m^2/kg) and apparent magnitude (mag) of the selected objects of the AIUB catalogue

NAME	E	I	A	A/M	Mag
E08241A	0.040	13.26	43200	1.20	16.1
E06321D	0.036	7.0	42900	2.56	15.3
E07194A	0.026	6.76	42000	3.31	16.8
E07308B	0.233	6.52	436008.93	15.9	
E06293A	0.092	11.89	44000	15.30	16.8

corresponds to a full absorption (other implementations use the formula for the radiation pressure without the factor of $\frac{1}{2}$, in those cases a factor of 1 for the reflection coefficient corresponds to full absorption). A/m is the area-to-mass ratio. The value for the DRP and therefore for the AMR is assumed to be constant over the whole fit interval of observations in orbit determination as well as in propagation.

Five objects have been chosen for a detailed investigation. All objects were discovered and first detected by the AIUB and are not listed in the USSTRATCOM catalogue. All of the objects are faint debris objects, they were followed over several years, and no maneuvers were detected. A current set of orbital elements and an average value for the apparent magnitude are listed in Tab. 1.

All objects are in GEO-like orbits, except E07308B has an eccentricity significantly different from zero. For the orbit determination, a specific controlled setup was chosen. Two sets of observations were chosen, at the end and at the beginning of each fit span. To find reliable orbits, the observation sets span a time interval of at least 1.2 hours. A reliable orbit is defined as an orbit which produces small residuals in propagation; see [3] for further details. Each set of observations consist of four to eight single observations. The overall fit span in between the sets spans between 10 and 120 days. Although the fit spans are quite different, the orbits are comparable in accuracy of propagated orbits in this specific setup; see [3] for further details.

The orbits were first determined with observations from one observation site only, then with combined observations from different sites in the setup mentioned above. The observations used in this investigation stem from the ESASDT, ZIMLAT, and from several telescopes of the ISON network, provided courtesy of the Keldish Institute of Applied Mathematics, Moscow, which supported this work in offering observations from additional sites.

The controlled setup was chosen, to ensure comparable orbits. In such a setup, possible error sources can be closely monitored. The risk of introducing variations that might display in the AMR values is minimized. A sparse data sampling as in the chosen setup, with larger gaps in between observation sets is a realistic output of optical observations.

4 EVOLUTION OF ORBITAL ELEMENTS

In the first step, the evolution of the orbital elements over time is inspected. In Fig. 1, the inclinations and errors in inclination, as determined in orbit determination, of the five objects are displayed. In most of the cases, the error bars are so small, that they are not visible in the plot. In all cases, the solutions are closely aligned to each other, only in the case of object E08241A in Fig. 1 can some spread in the data be observed. The orbits from the different observation sites produce nearly identical values. The expected decline and increase in the value of the inclination can be observed for all objects. For object E06293A, which has the highest AMR value, the inclination seems not to follow a steady increase over time, but some smaller periodic substructure seems to be superimposed. This may be due to the fact, that in this AMR region, the effect of the DRP is dominating over purely gravitational effects in the evolution of the orbit.

In Fig. 2 the evolution of the eccentricity values over time and the errors of eccentricity, as found in orbit determination for the different objects, are displayed. Periodic variations can be observed for all objects. Again, the different orbits with observations from one site only or from combined sites results in the same eccentricity values.

5 EVOLUTION OF AREA-TO-MASS RATIO

In Fig 3, the different AMR values for the different objects and observation sites are displayed. The error bars show the error in the determined DRP parameter. In all cases, the values for the AMR are not as nicely aligned as was the case for the orbital elements in Fig. 1 and Fig. 2.

For object E08241A, the area-to-mass values seem to form a cloud of values (see Fig. 3(a)), varying around a mean

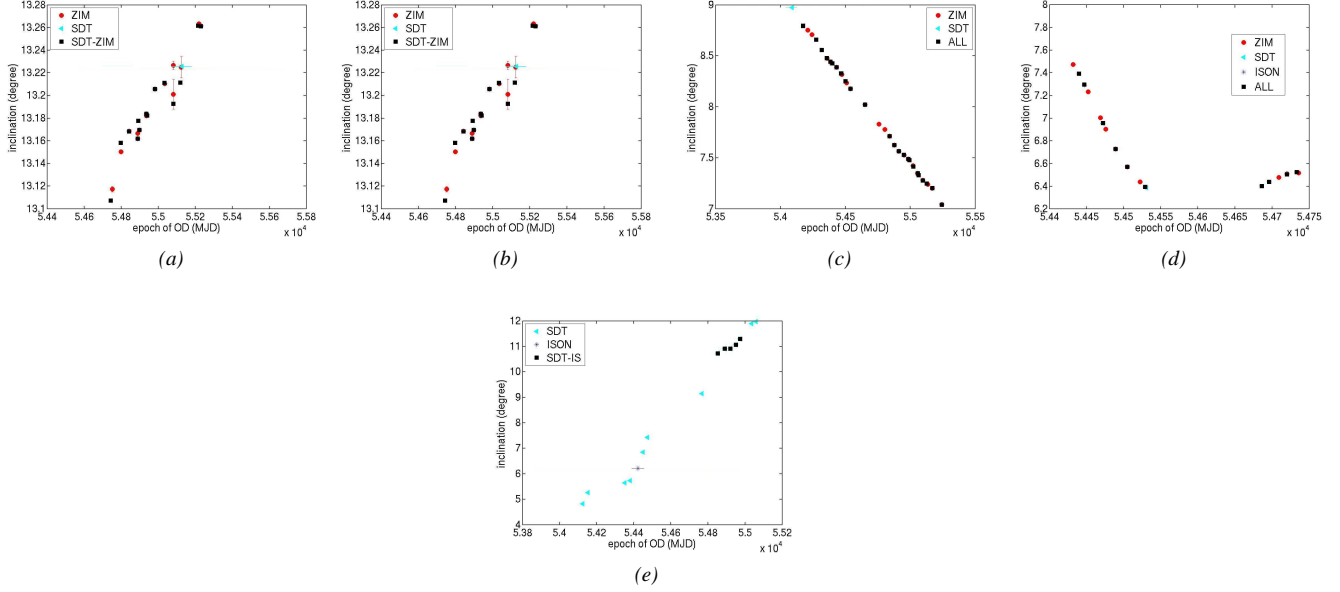


Figure 1: Inclination as a function of time for orbits of the object (a) E08241A, (b) E06321D, (c) E07194A, (d) E07308B, (e) E06293A.

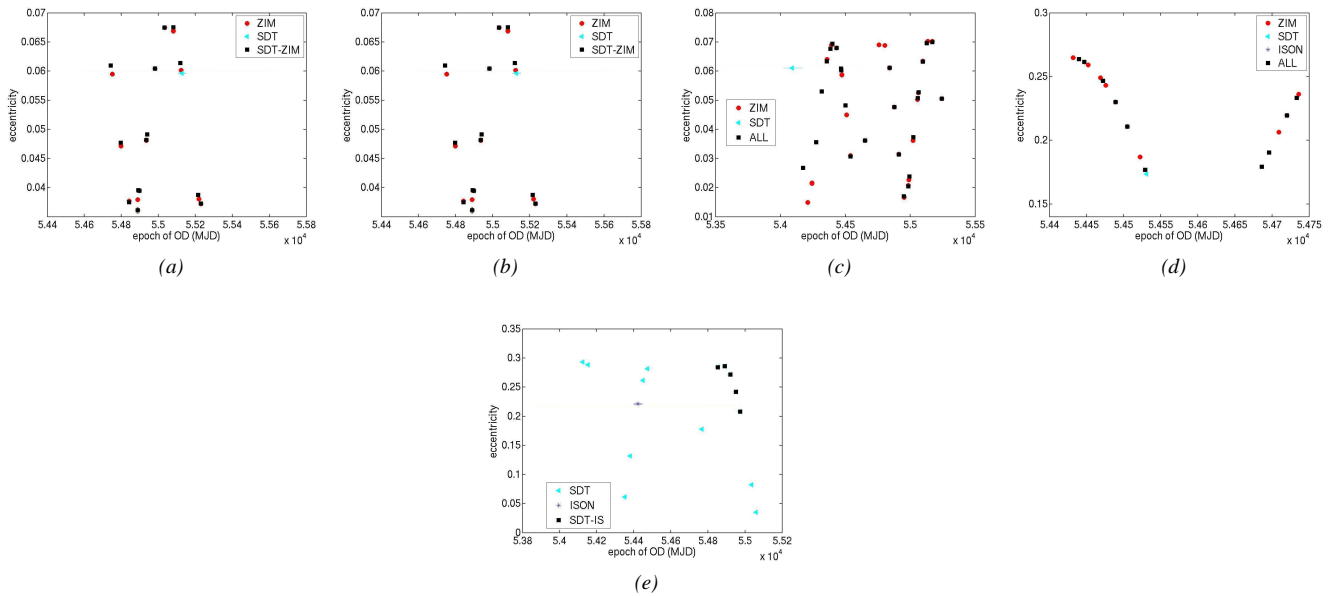


Figure 2: Eccentricity as a function of time for orbits of the object (a) E08241A, (b) E06321D, (c) E07194A, (d) E07308B, (e) E06293A.

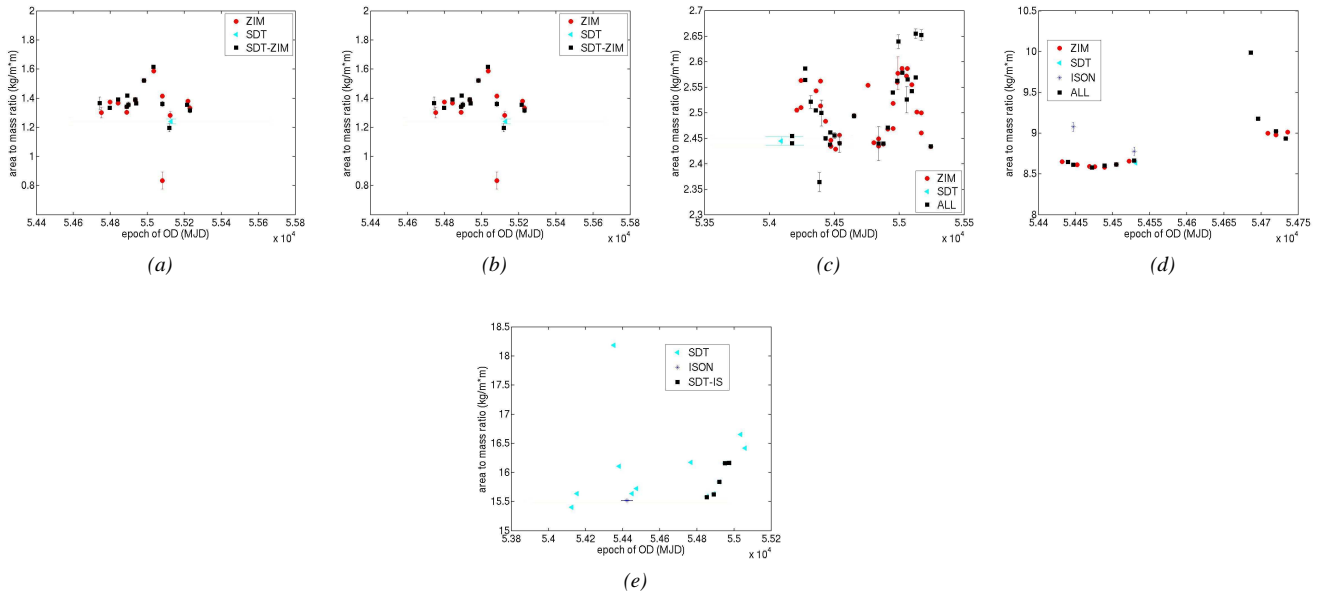


Figure 3: Area-to-mass ratio as a function of time for orbits of the object (a) E08241A, (b) E06321D, (c) E07194A, (d) E07308B, (e) E06293A.

value of 1.4 kg/m^2 . But a single value found in the orbit determination with Zimmerwald observations only, has a value of around 0.8 kg/m^2 .

For object E06321D (see Fig. 3(b)), the AMR value even seems to vary periodically around a value of 2.5 kg/m^2 , but also values of 2.35 kg/m^2 and 2.65 kg/m^2 occur. The AMR value of object E07194A (see Fig. 3(c)) seems to form a cloud around 3.5 kg/m^2 , but in the orbits determined with combined observations from all the sites, also values of 4.5 kg/m^2 and 2.3 kg/m^2 can be found.

Object E07308B (see Fig. 3(d)) seems to generally increase its AMR value over time from a value of 8.5 kg/m^2 up to 9.0 kg/m^2 . But single orbits also show AMR values of i.e. 10 kg/m^2 .

For the object with the largest AMR, which is investigated in this paper, E06293A, there may also a periodic variation over time detected, with a general trend to increasing values over time (see Fig. 3(e)), increasing from 15.310 kg/m^2 to 16.510 kg/m^2 . But one orbit determined with ESASDT data also shows a value of 18.210 kg/m^2 .

To gain more insight, all orbits were propagated and compared to further observations of the same object, which were not included in the orbit determination process with the COROBS tool. The additional observations were all cross checked by further dense data orbit determinations; they serve as a ground truth. For further details, see [4]. In Fig. 4 the residuals determined between the predicted ephemeris from orbit propagation to the observed positions in degrees on the celestial sphere are displayed. The values are mean values over all residual values found 50 days after orbit determination and their standard deviations as error bars.

Fig. 4(a) shows, that for object E08241A, one orbit produces large residuals of 1 degree, but this orbit does not show *unusual* orbital parameters or AMR value. The orbit with Zimmerwald data, which produced the *outlier* AMR value, does not show up prominently in the residual plot.

In Fig. 4(b), which shows the residuals of object E06321D, several orbits determined with combined observations from the Zimmerwald, ESASDT, and ISON data, show large standard deviations in the residuals, although the mean value of the residuals is well under 0.2 degrees. Three of the orbits could be identified to be the four AMR values in Fig. 3(b), which seems not to follow the periodic variation trend; the orbit with the largest variation, however, with an AMR value of 2.45 kg/m^2 , seems to (coincidentally?) fit into the periodic variations of the AMR value. A similar observation can be made in Fig. 4(c) in comparison with Fig. 3(c). The orbits determined with the observations from all sources that do not show large overall residuals are the ones that have significantly higher and smaller AMR values than the other orbits. The orbits with the highest residuals in Fig. 4(c), do show similar AMR values with the other orbits.

A similar trend can be observed in Fig. 4(d), for object E07308B, for the two orbits out of the ISON observations, that showed up significantly in Fig. 3(d). They also show the largest standard deviations in Fig. 4(d). But the orbit, which has

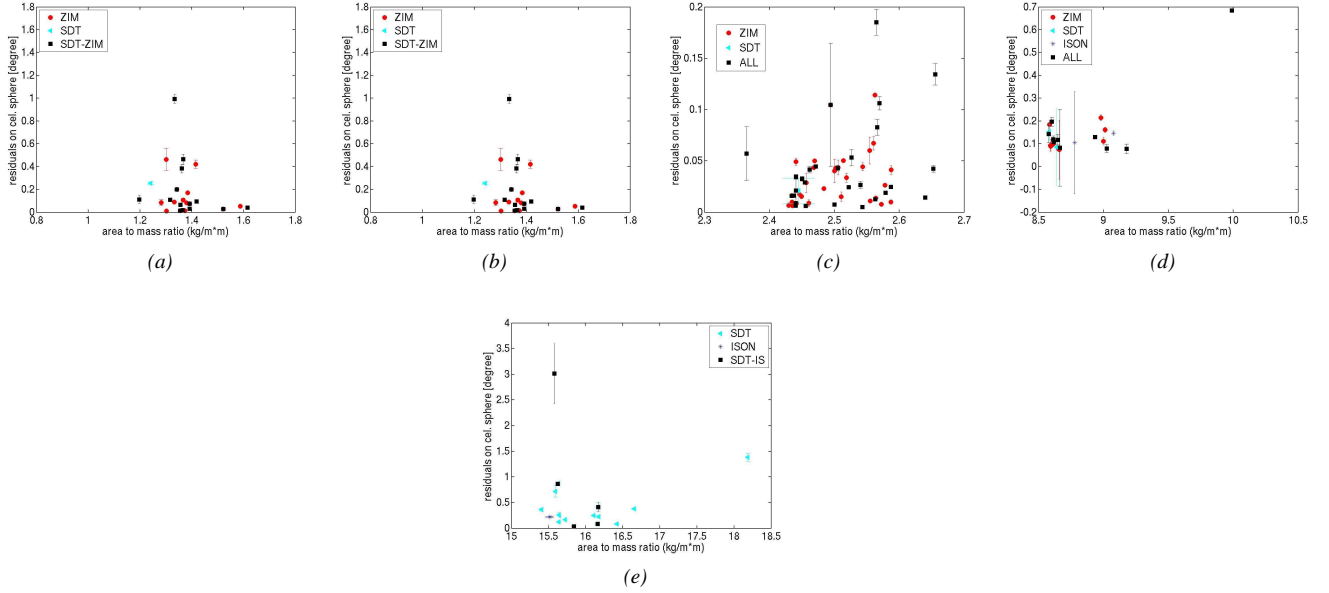


Figure 4: Residuals of propagated orbits on the celestial sphere as a function of area-to-mass ratio for orbits of the object (a) E08241A, (b) E06321D, (c) E07194A, (d) E07308B, (e) E06293A.

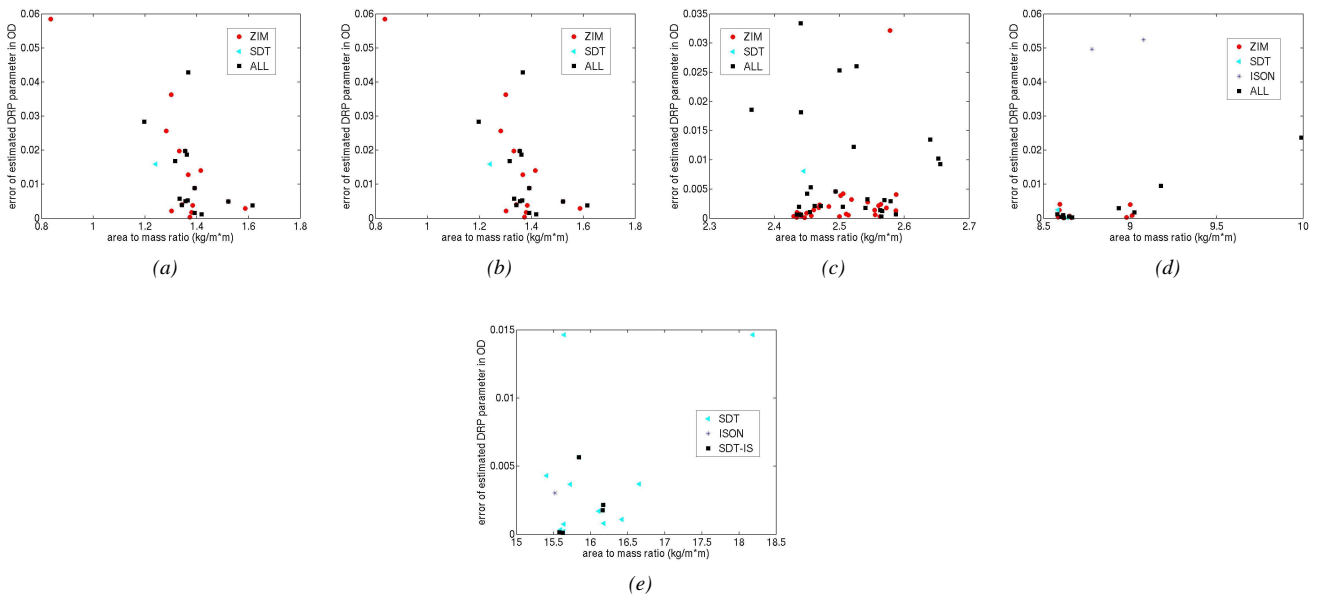


Figure 5: Error in the DRP parameter as found in orbit determination as a function of area-to-mass ratio for orbits of the object (a) E08241A, (b) E06321D, (c) E07194A, (d) E07308B, (e) E06293A.

the largest offset compared to the mean AMR value, does not show a large standard variation. The orbit with the AMR value of 10 kg/m^2 has the largest residual for all orbits regarded here, of 0.7 degrees. Object E06321D shows one orbit from combined observations of the ESASDT and ISON data, which shows a very large residual with 3 degrees and large standard variation, but the value does not show a significant value for the AMR. The orbit out of the ESASDT observations, however, also shows a relatively large residual of almost 1.5 degrees but no large variations.

In the final step, the dependency of the AMR value on the error in the DRP parameter, as it was found in orbit determination, was investigated. For object E08241A, Fig. 5(a) shows that the orbit, which has far the smallest AMR value, also shows the largest DRP error, nevertheless, the absolute value of 0.06 is very small. The same situation can be observed for object E07308B in Fig. 5(d) and for object E06293AB in Fig. 5(e). The area-to-mass ratios, which are far off the mean value, show the largest DRP errors, but the absolute values are also below 0.06.

For object E06321D, Fig. 5(b) shows very small DRP errors overall, with most of the orbits below 0.01. For object E07194A, however, the orbit with the largest DRP value does not show an unexpected AMR value. On the other side, the DRP error values for the orbits with unexpected AMR values have small DRP errors.

6 CONCLUSIONS

Five objects in GEO-like orbits, with area-to-mass ratio values of 1 kg/m^2 , up to 15 kg/m^2 have been investigated. The objects were discovered and orbits were maintained over several years by the AIUB. Under a controlled setup, orbits were determined with the CelMech tool from observations of single sites and of combined observations from different sites. The controlled setup was chosen to be able to acquire comparable orbits over time, to monitor all possible error sources and to minimize the risk to introduce variations in the AMR value by the sheer choice of observations.

The orbital elements were found to be consistent for all objects. No differences between the orbits from the different observation sites or the orbits from combined observations could be observed.

The AMR values of all objects showed variations. Some indicated a constant increase of the area-to-mass ratio value, while others indicated a periodic variation. In general, all variations were approximately 20 percent around the mean value for this object. However, all objects also showed single orbits with AMR values far larger and/or smaller than this 20 percent, which did not follow the general trend in the evolution of the AMR value observed in the majority of orbits.

Some of the orbits of these outliers showed either large residuals in the propagated orbits, when compared to further optical observations with the COROBS tool. Some of them showed a small mean value of the residuals, but large standard deviations in the residuals. Others showed larger values in the error of the DRP parameter, which has been determined in orbit determination, but the overall values were still relatively small. But orbits with insignificant AMR values could also show either larger mean values of the residuals, or large standard variation of the residuals or large DRP values.

It can be concluded that there obviously seem to be variations in the current AMR values of space debris objects. Their investigation is complex and no general rule, valid for all orbits, could be found.

7 ACKNOWLEDGMENTS

The work was supported by the Swiss National Science Foundation through grants 200020-109527 and 200020-122070.

The observations from the ESASDT were acquired under ESA/ESOC contracts 15836/01/D/HK and 17835/03/D/HK.

REFERENCES

- [1] R. Musci. Analyzing long Observation Arcs for Objects with high Area-to-Mass Ratios in Geostationary Orbits. In *Proceedings of the International Astronautical Congress 2008, A6.1.10, Glasgow, Scotland, Great Britain, 29 Sep- 3 Oct, 2008*, 2008.
- [2] G. Beutler. *Methods of Celestial Mechanics*. two volumes. Springer-Verlag, Heidelberg, 2005. ISBN: 3-540-40749-9 and 3-540-40750-1.
- [3] C. Früh. Orbit Propagation and Validation with Angle-Only Observations. In *Proceedings of the 20th AAS/AIAA Astrodynamics Specialist Conference, Toronto, Canada, August 2nd - 5th, 2010*, volume Toronto, Canada, 2010.
- [4] C. Früh, T. Schildknecht, R. Musci, and M. Ploner. Catalogue Correlation of Space Debris Objects. In *Proceedings of the Fifth European Conference on Space Debris, ESOC, Darmstadt, Germany, 30 March-2 April 2009*, 2009.